Desalination and Water Treatment
www.deswater.com
doi: 10.1080/19443994.2015.1075159

57 (2016) 15941–15951
July

Taylor & Francis
Taylor & Francis Group

Trichlorophenol removal from aqueous solutions by modified halloysite: kinetic and equilibrium studies

Sousna Sahnoun, Mokhtar Boutahala*, Hassina Zaghouane-Boudiaf, Larbi Zerroual

Laboratoire de Génie des Procédés Chimiques (LGPC), Faculté de Technologie, Département de Génie des Procédés, Université Ferhat Abbas Sétif-1, Sétif 19000, Algeria, Tel./Fax: +213 36 83 49 74; emails: ssnsahnoun@yahoo.fr (S. Sahnoun), mboutahala@yahoo.fr (M. Boutahala), boudiafhassina2000@yahoo.fr (H. Zaghouane-Boudiaf), zerroual@yahoo.fr (L. Zerroual)

Received 11 July 2014; Accepted 15 July 2015

ABSTRACT

To obtain new materials, we modified Algerian halloysite by thermal activation (HalC), acid activation (HalA), combined thermal-acid activation (HalCA) and acid-thermal activation. X-ray diffraction, Fourier Transform infrared and BET textural analysis were used to characterize changes. After the HalC of halloysite at 600˚C, no XRD peaks were shown and a total disappearance of the absorption bands ranging from 3,700 to 3,600 cm^{-1}. The treatment of halloysite by sulphuric acid increases the surface area from 185.4 to 321.0 m^2/g. Halloysite is first calcined and then activated by acid, its surface area increases from 74.3 to 538.6 m^2/g. The effect of initial pH, adsorbent dose, contact time and temperature on the removal of 2,4,5-trichlorophenol (TCP) by modified halloysite samples was investigated. Equilibrium data were fitted to the Langmuir, Freundlich and Toth models. The best fit of the cited models was the Freundlich model, which suggested infinite adsorption onto heterogeneous surface. The pseudo-first-order, pseudo-second-order and intraparticle diffusion models were applied to the experimental kinetic data. The results showed that the pseudo-second-order is the best model to describe the process. The study of thermodynamic parameters shows that the process of adsorption of TCP onto the prepared samples was spontaneous, endothermic and physical in nature.

Keywords: Halloysite; Acid activation; Thermal activation; Characterization; Removal; Trichlorophenol

1. Introduction

Chlorophenols are mainly produced in chemical industries, such as petroleum refineries, plastics, pharmaceuticals and pesticides [1]. The 2,4,5-trichlorophenol (TCP) is mainly used as a fungicide in the production of paper and as a precursor in the herbicide industry [2]. Low levels of TCP were found in drinking water, it presents a hazard both to human health and to the environment [1]. Various physical and chemical methods have been employed for the treatment of chlorophenols, including photo-oxidation [3], electrochemical oxidation [4], ultrafiltration [5] and adsorption [6–8]. The last process is the most widely used due to its relatively simple implementation and low operation cost. In recent years, there have been many investigations, with the aim of finding effective adsorbents for the treatment of phenolic aqueous wastes. The clay minerals were reported to be

*Corresponding author.

unconventional adsorbents for the removal of chlorophenols from aqueous solutions [9–11]. They have advantages over commercially available adsorbents in terms of low cost, abundant availability, high adsorption properties, non-toxicity and large potential for ion exchange. Utilization of locally available clays could bring massive economic and environmental benefits to wastewater industries. Halloysite nanotubes are a kind of aluminosilicate clays with hollow nanotubular structure mined from natural deposits. It possesses a regular nanotubular morphology, bulk structure and rich mesopores and nanopores [12,13].

The structure and chemical composition of halloysite are similar to those of kaolinite, but halloysite can be intercalated by a monolayer of water molecules giving a basal spacing near 10 Å [14]. Halloysite occurs mainly in two different polymorphs, the hydrated form (basal distance around 10 Å) with the $Al_2Si_2O_5(OH)_4{\cdot}2H_2O$ formula and the dehydrated form (basal distance around 7 Å) with the $Al_2Si_2O_5(OH)_4$ formula, which is identical to kaolinite. Recently, it was used as nanocomposites, nanocontainers and adsorbents [15–18]. The objectives of this study were to characterize the surface modification of an Algerian halloysite (Hal) after calcination, activation and combined acid and thermal activation (HalC). In addition, these solids currently known as compounds presenting high resistance towards oxidation reactions were applied for removing TCP from aqueous solutions.

2. Materials and methods

2.1. Materials

2.1.1. Raw halloysite

Hal was directly collected from a mine of Djebbel Debbagh (Guelma), milled, sieved and dried at 100°C for 24 h. The chemical composition of the halloysite in weight is: 46.34% SiO_2; 37.96% Al_20_3; 0.05% Fe_2O_3; 0.83% CaO; 0.08% MgO; 0.02% K_2O; 0.02% Na_2O; 1.25% MnO_2; 13.45% loss on ignition (1,000°C for 1 h) [13].

2.1.2. Activation of raw halloysite

2.1.2.1. Thermal activation. The raw material was dried at 100°C for 24 h and left to cool at room temperature in a desiccator. The HalC of Hal was performed by heating the samples at 600°C for 2 h under air in a muffle furnace at a rate of 10°C/min, and thereafter were cooled and stored in air-tight plastic bottles in a desiccator for further use. The thermal-activated sample was noted as HalC.

2.1.2.2. Acid activation. The acid activation of Hal was carried out in a rotary shaker with temperature and agitation control. Hal was treated with 1 M H_2SO_4 at 90°C for 6 h. The acidified halloysite was then washed several times with double-ionized water till SO_4^{2-} ion was undetectable in the supernatant using barium chloride solution. The final sample was centrifuged with Beckman centrifuge and dried at 60°C for 18 h, and stored in air-tight plastic bottles in a desiccator for further use. The acid-activated sample was noted as HalA.

2.1.2.3. Thermal and acid activation. The thermal and acid activation of Hal followed a two-step procedure. In the first step, Hal was calcined at 600°C for 2 h. The HalC was further subjected to acid activation with 1 M H_2SO_4 at 90°C during 6 h. The sample was exhaustively washed until SO_4^{2-} were undetectable. The sample was then cooled and stored in air-tight plastic bottles for further use.

The obtained sample was named as combined thermal-acid activation (HalCA).

2.1.2.4. Acid and HalC. The acid and HalC of Hal followed a two-step procedure. In the first step, we used acid activation which is described in Section 2.1.2.2, in the second step we calcinated the HalA sample as described in Section 2.1.2.1. The obtained sample was noted as HalAC.

2.2. Trichlorophenol (TCP)

The TCP supplied by Sigma–Aldrich Chemicals was used as an adsorbate. TCP has a molecular weight of 197.45 g/mol and linear formula: $Cl_3C_6H_2OH$. Its solubility in water at 20°C is 900 mg/L and it has a pK_a between 6.7 and 6.94. The TCP solutions were prepared in the neutral distilled water from an initial solution of 500 mg/L of TCP for all experiments. Their pH was adjusted between 2 and 10 by adding either 0.01 N HCl or 0.01 N NaOH solutions.

2.3. Characterization techniques

X-ray diffraction (XRD) analysis for the halloysite samples was conducted using a Bruker D8 advance diffractometer operating at 40 kV and 30 mA with Cu K_α radiation ($\lambda = 0.15418$ nm). Radial scans were recorded in the reflection scanning mode from $2\theta = 5$ to 80° with a scanning rate of 10°/min. Bragg's law, defined as $n\lambda = 2d \sin \theta$, was used to compute the crystallographic (d) for the examined clay samples.

FT-IR study was carried out using Fourier Transform infrared (FTIR) 8400S Shimadzu having a standard mid-IR DTGS detector. FT-IR spectra were recorded in the range of 400–4,000 cm^{-1} using KBr pellets technique.

Nitrogen gas adsorption–desorption isotherms were measured using a Micromeritics Tristar 3000 instrument at 77 K. The measurements were made after degassing the samples under vacuum at 200°C for 3 h. The specific surface areas are determined according to the BET method at the relative pressure in the range of 0.05–0.35 [19]. The total pore volumes of micro and mesopores were directly determined from the Nitrogen adsorption at $P/P_o = 0.98$. The pore size distribution is calculated using the Barret–Joyner–Haleda (BJH) method using the desorption isotherm [20].

The point of zero charge (pH_{pzc}) of all halloysite samples used for the adsorption is determined using solid to liquid ratio of 1:1,000. For this, 0.1 mg of halloysite is added to 100 mL of water with varying pH from 2 to 12 and stirred for 24 h. The final pH value of the solution is plotted against initial pH of the solution [21].

The CEC of the raw halloysite and modified halloysite was calculated using bis-ethylenediamine copper(II) ($[Cu(en)_2]^{2+}$) complex method [22,23].

2.4. Adsorption experiments

Adsorption experiments were carried out in a batch equilibrium mode. The effect of the initial TCP concentration of 120 mg/L was investigated. An amount of modified halloysite (50 mg) was dispersed in 50 mL of TCP solution and stirred with an agitation speed of 100 rpm. After each time of contact, the pH of solution was measured (it was found no significant change in pH) a sample was removed and centrifuged. The TCP concentrations were determined using a UV-1700 UV spectrophotometer at 290 nm. The amount of TCP adsorbed was derived from the initial and final concentrations of TCP in the liquid phases. All experiments were run in triplicate to ensure reproducibility. The TCP uptake by modified halloysite was calculated by the following equation:

$$q_t = \frac{(C_0 - C_t)\,V}{m} \quad (1)$$

where q_t is the amount of adsorbed TCP at time t (mg/g); V the volume of solution (L); C_0 and C_t are the initial and at time t TCP concentration, respectively (mg/L); and m is the weight of adsorbent (g).

2.5. Adsorption isotherms

A constant volume of TCP solution 50 mL with varying initial concentrations (10–250 mg/L) was mixed with a constant amount of 50 mg. The dispersions were shaken at a temperature of 23 ± 1°C, under an agitation speed of 100 rpm which was optimized. The dispersions were maintained at a constant pH 2 value over 120 min. The TCP q_e loading (in mg per unit weight of sample) was obtained using the following equation:

$$q_e = \frac{(C_0 - C_e)\,V}{m} \quad (2)$$

where C_0 and C_e (mg/L) are initial and equilibrium TCP concentrations, respectively; V (L) is the volume of the solution; and m (g) is the adsorbent mass; and q_e is the adsorption capacity at equilibrium.

3. Results and discussion

3.1. Characterization of materials

XRD (Fig. 1) is used to follow the structural alterations resulted from thermal, acid and both thermal and acid activation. The d_{001} and d_{002} diffractions of Hal are seen at 12.32 and 20.20° (2θ), with the distances of 7.2 and 3.6 Å, which are typical characteristic peaks of dehydrated halloysite $Al_2Si_2O_5(OH)_4$. The feature of the X-ray pattern of halloysite having common tubular morphology is the very intense reflection at 4.4 Å, this reflection is observed at about 20° with relative intensity of 100%. The peaks of quartz are detected at 2.96 and 2.45 Å [12]. The reflexions of the original halloysite phase became narrower after acid

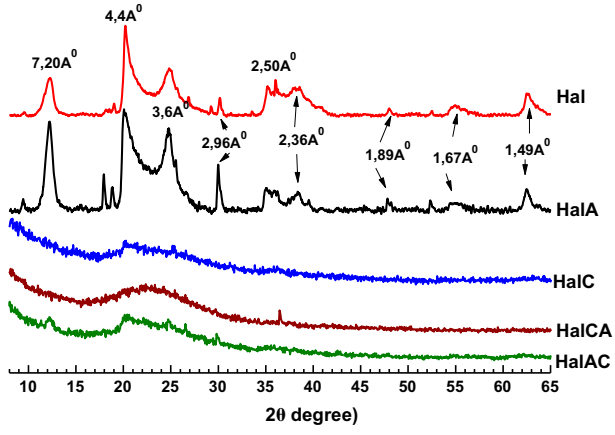

Fig. 1. Powder XRD patterns for raw and modified halloysites.

activation (HalA). The narrowing of the peak may be related to the increase in crystallite size and/or the decrease in the mean lattice strain. This indicates that the halloysite phase is more ordered in the acid-treated materials, and the high content in octahedral Al of halloysite makes it, especially resistant to acid attack [24]. When halloysite sample (Hal) was calcined at 600°C for 2 h (HalC) dehydration occurred, the peaks of halloysite disappeared, and little amount of an amorphous phase, that some authors ascribe to an amorphous phase of SiO_2 [25], began to separate as evidenced by the presence of a very broad band between $2\theta = 10° - 40°$. Heating halloysite above 550°C transforms it into metakaolin (HalC) by the effect of the loss of structural OH groups and a rearrangement in Si and Al atoms leading to a decrease in octahedral Al and the appearance of penta-and tetra-coordinated Al [26]. When HalC sample was activated with sulphuric acid at 90°C, for 6 h (or HalA was calcined at 600°C, for 2 h) no other differences were observed in the XRD patterns of HalC sample. It was proposed that, metakaolins possess more penta-and tetra-coordinated Al, and are thus more easily attacked; in fact, the acid treatment can convert them into materials of acidity comparable to that of acid-activated montmorillonite [26].

The FTIR spectra of all halloysites are shown in Fig. 2. Changes in the halloysite hydroxyl surface upon different treatments can be followed in the hydroxyl stretching region, as well. The Hal has two infrared active modes centred at 3,694, and 3,619 cm^{-1}. The two higher frequency vibrations are assigned to the stretching vibration due to external and internal O–H groups of halloysite [27]. After acid treatment of Hal, the resolved OH stretching bands show a slight

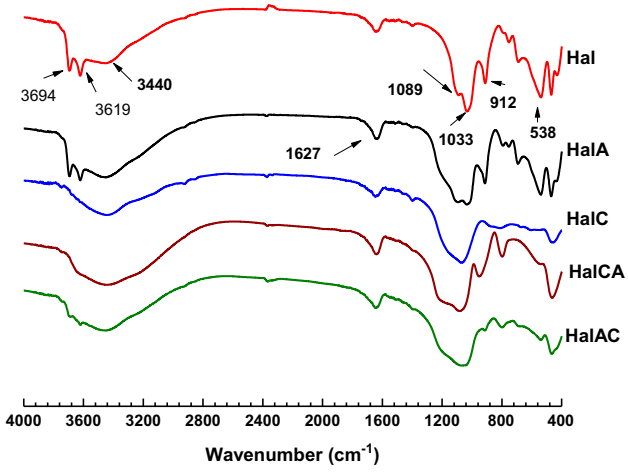

Fig. 2. FTIR spectra for raw and modified halloysites.

increase. For halloysite (HalC, HalCA and HalCA), we observed a complete disappearance of the bands in the zone with wavelength ranged between 3,700 and 3,600 cm^{-1}, which confirms the dehydroxylation and the absence of octahedral Al due to the thermal treatment at 600°C. The broad absorption bands, centred at 3,440 cm^{-1} were attributed to the physisorbed water molecules. The H–O–H bending band vibrations of adsorbed water are centred at 1,627 cm^{-1}. This band is more intense and broader in halloysite in comparison with Kaolinite [28]. Quartz is also detected at 2,366 cm^{-1} [13]. The structural O–H bending vibrations and the Si–O stretches exist in the region 1,300–440 cm^{-1}. The 1,114 cm^{-1} shoulder is assigned to stretching mode of apical Si–O, while the bands at 1,089 and 1,033 cm^{-1} are caused by the stretching vibrations of Si–O–Si. The band at 912 cm^{-1} is caused by bending modes of Al–O–H [29]. After thermal treatment, the Al–OH (912 cm^{-1}) and Si–O–Al (538 cm^{-1}) vibration bands are suppressed, due to the distortion in the tetrahedral and octahedral sheets and the appearance of metakaolin. New bands at 1,065 cm^{-1} (Si–O) and at 476 cm^{-1} (O–Si–O) in metakaolin appeared [30].

The N_2 adsorption–desorption isotherms of Hal and modified halloysites are presented in Fig. 3(A). The isotherms of these samples are classified as type II on the basis of IUPAC recommendations; this isotherm is typical of mesoporous structures. The hysteresis loop of these samples is similar to type H3, typical agglomerates of plate-like particles containing slit-shaped pores [31]. The isotherms also suggest the presence of some micro-porosity and macro-porosity. Table 1 shows the specific surface areas, micropore and mesopore volumes, of the studied solids. After the treatment by acid, the BET surface area of halloysite increases from 185.4 to 321.0 m^2/g, the total volume also changes from 0.21 to 0.39 cm^3/g. The treatment by acid leads to an increase in the amount of micropores and mesopores. On the other hand, in the case of calcinated halloysite the area decreases from 185.4 to 74.3 m^2/g and the total volume decreased too. We clearly see that the surface changes with the mode of treatment. These changes are probably caused by a disaggregation of clay particles, elimination of mineral phases (quartz and calcite) and dissolution of the external layers, thus altering the chemical composition and the structure of the clay [26]. By cons, halloysite that has undergone during the first step calcination, then acid activation, the surface area ranges from 74.3 to 538.6 m^2/g. This increase in surface area is due to the increase in the porosity. The pore size distribution of untreated halloysite samples shows a sharp peak at a radius of 3.8 nm (Fig. 3(B))

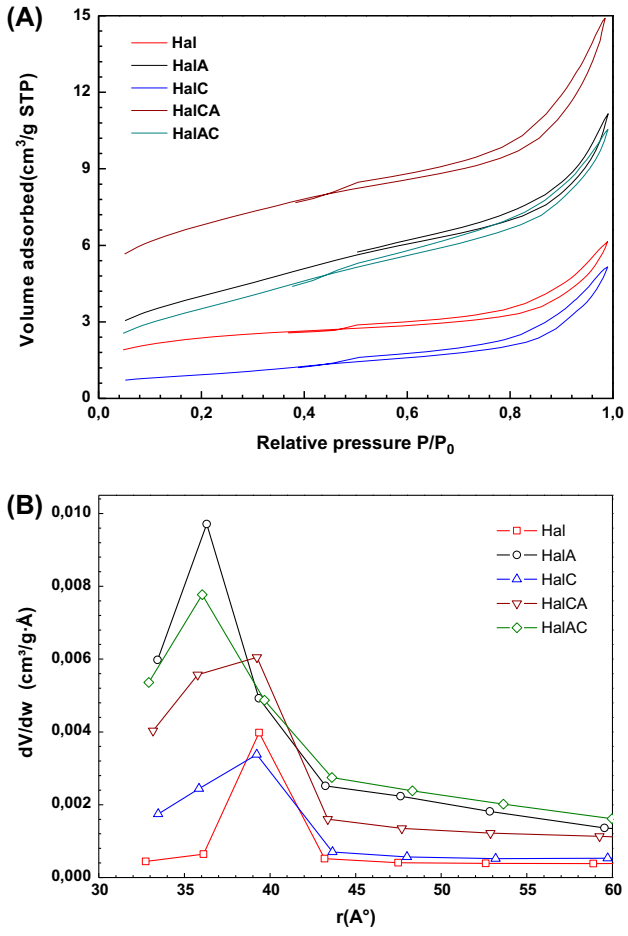

Fig. 3. Nitrogen adsorption-desorption isotherms (A) and pore size distribution curves and (B) of the halloysite samples.

and thus is mesoporous. The acid treatment changed the pore size distribution where the sharp peak curve vanished indicating the decrease in the number of pores with diameter 3.8 nm and increase in the number of pores with diameter <3.8 nm.

From the graph (figure not showed), the pH_{pzc} values obtained for the halloysite samples were comprised between 3 and 7.1 (see Table 1), indicating that their surfaces were more on the acidic group. Similar results were reported by Levis and Deasy [12] and Mellouk et al. [13]. The surfaces of halloysites are positively charged when solution pH is below pH_{pzc}; while they acquire a negative charge when solution pH is above the pH_{pzc} [21]. The reason for the generation of the negative surface charge can be attributed as follows: the surface of halloysite bean abundant Si–OH and Al–OH; which can ionize in the following form:

$$Si/Al - OH_2^+ \overset{H^+}{\longleftarrow} Si/Al - OH \overset{OH^-}{\longrightarrow} Si/Al - O^- \quad (3)$$

The CEC values of the raw and modified halloysite samples indicated in Table 1 are very low. This behaviour can be explained by the effect of the treatment procedure. In fact, the acid activation provokes a small decrease in the CEC value because sulphuric acid attacks the aluminium contained in the octahedral layers. In the case of calcination, the decrease in the CEC value is more important. This is due to the removal of hydroxyl groups and water molecules from halloysite, which leads to a decrease in the interlayer space.

3.2. Effect of pH on TCP adsorption

The pH value of the solution was an important controlling parameter in the adsorption process, since it influences the electrostatic interaction between the adsorbent and the adsorbate. These forces are of paramount importance in the removal of a weak electrolyte such as TCP. The pH of the solution may change: the surface charge of the adsorbent, the degree of ionization of the adsorbate molecule and the extent of dissociation of functional groups on the active sites of the adsorbent [32]. The adsorption of TCP was studied over a pH range between 2 and 10 by adding adequate amounts of NaOH or HCl diluted

Table 1
Surface areas and porosity characteristics of the halloysite samples

Samples	S_{BET} (m^2/g)	S_{ext} (m^2/g)	S_{mic} (m^2/g)	V_{tot} (cm^3/g)	V_{mic} (cm^3/g)	D_p (nm)	pH_{pzc}	CEC mmol/100 g
Hal	185.4	44.1	141.3	0.21	0.07	11.5	7.1	4.9
HalA	321.0	136.0	184.9	0.39	0.12	8.2	3.2	3.9
HalCA	538.6	118.2	420.4	0.52	0.21	9.6	3.0	3.4
HalAC	285.8	144.1	141.7	0.37	0.09	7.8	5.2	1.9
HalC	74.3	54.8	19.5	0.18	0.01	10.3	5.9	1.5

Note: $D_p = (4\ V/A)$.

solutions to the initial unbuffered solution containing the phenolic compound. Fig. 4 shows that the adsorption capacity of TCP onto halloysite samples decreases significantly with the increase in the pH. The maximum removal of TCP for a contact time of 120 min was at pH 2. According to Eq. (3), when solution pH is lower than the pH_{pzc}, the total surface charge would be in average positive, whereas at a higher solution pH, it would be negative. The TCP uptake was the highest at lower pH, where the pH was below the pK_a of TCP. At acidic pH, the concentration of unionized chlorophenol species is high and decreases with increasing pH and the dispersive interactions between the positively surface samples and TCP molecules predominated [32]. However, when pH solution is above the pK_a of TCP, the concentration of anionic species of TCP was high. It increases with increasing solution pH and uptake of TCP decreases due to the electrostatic repulsions between the negative surface charge and the chlorophenolate anions and between chlorophenolate–chlorophenolate anions in the solution. Similar trends were reported in the literature for the adsorption of 2,4,6-tricholorophenol on activated clay [32] and coconut shell-based activated carbon [33] as well as adsorption of 4-chlorophenol and 2,4-dichlorophenol on anaerobic granular sludge [34]. From the experimental results, pH 2.0 was selected as an optimum pH value.

3.3. Effect of adsorbent dose

Adsorbent dose is an important parameter in the determination of adsorption capacity. The effect of the adsorbent dose was investigated by the addition of various amounts of all halloysite samples in 50 mL TCP aqueous solution with a concentration value of 100 mg/L at 25°C for 2 h. The result is shown in Fig. 5. It was observed that q_e amount adsorbed (mg/g) decreases with an increase in adsorbent dose from 10 to 300 mg for all samples. We also note that HalCA sample is more effective in eliminating the TCP. This can be attributed to the increase in the adsorbent specific surface area and structure porous and availability of more adsorptions sites [18]. Consequently, the adsorbent dose was maintained at 50 mg in all subsequent experiments, which was considered to be sufficient for the removal of TCP.

3.4. Kinetics of adsorption

The effect of contact time on the removal rate of TCP on halloysite samples is shown in Fig. 6. The concentration decay curves show that the removal of TCP steadily increased with time and lasts around 40 mn to reach equilibrium for all samples. The results revealed that the TCP adsorption was fast at the initial stages of the contact period, and thereafter it became slower near the equilibrium. We observe from the curves that the kinetics of adsorption of TCP by modified halloysites is very dependent on the nature of the sample. The distinct shapes of the concentration decay curves show different steps on the kinetic uptake, pointing out to the important role of the porous structure of the materials, and more specifically, to their meso/macroporous network. The declining trend of TCP removal was significantly much faster for the calcinated halloysites than for activated ones (with more developed porous features). To better understand

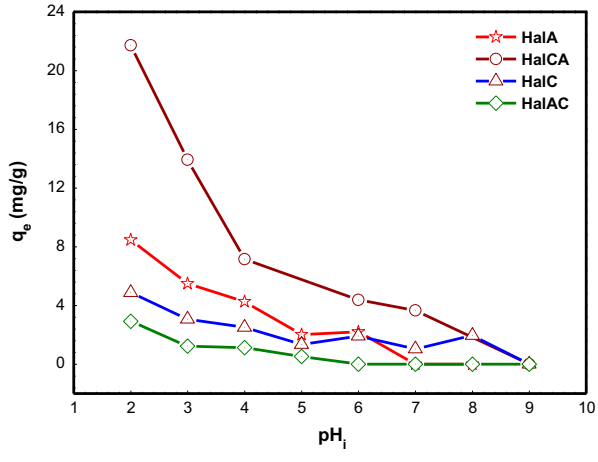

Fig. 4. Effect of initial pH on adsorption of TCP onto modified halloysite samples. (C_0 = 100 mg/L; adsorbent mass = 50 mg; T = 23 ± 1°C; V_{agi} = 100 rpm; V_{sol} = 50 mL).

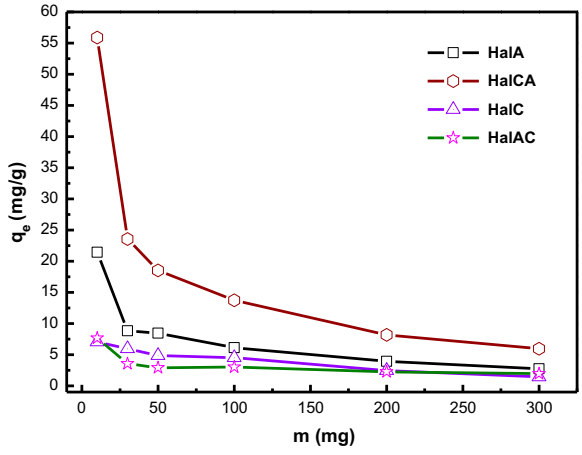

Fig. 5. Effect of adsorbent dose on adsorption of TCP onto modified halloysite samples. (C_0 = 100 mg/L; T = 23 ± 1°C; V_{agi} = 100 rpm; V_{sol} = 50 mL; pH 2).

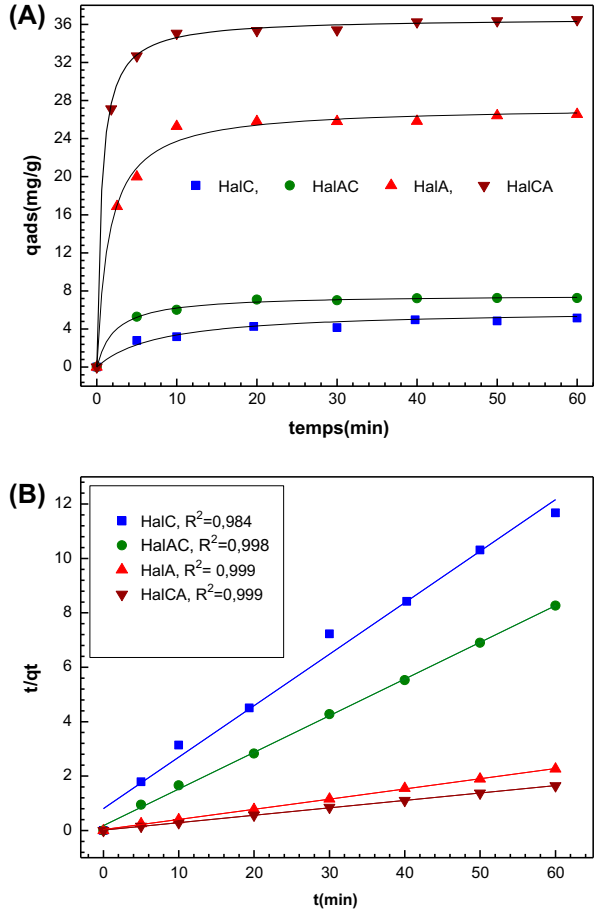

Fig. 6. The pseudo-second-order kinetics for adsorption of TCP onto modified halloysite samples. (C_0 = 100 mg/L, adsorbent mass = 50 mg, T = 23 ± 1 ℃; pH 2, V_{agi} = 100 rpm, V_{sol} = 50 mL) (A) nonlinear expression and (B) linear expression.

and analyse these differences, the kinetic data in this study were applied on pseudo-first-order and pseudo-second-order models [35,36].

First-order and pseudo-second kinetics model can be expressed as Eqs. (4) and (5), respectively:

$$\frac{dq_t}{dt} = k_1(q_e - q_t) \tag{4}$$

$$\frac{dq_t}{dt} = k_2(q_e - q_t)^2 \tag{5}$$

where q_e and q_t are the adsorption capacities at equilibrium and at time (min), respectively, and k_1 (min^{-1}) and k_2(g/mg/min) are the rate constants of first-order and pseudo-second kinetics adsorption, respectively. Often, these two equations were used in their linear form (Eqs. (6) and (7)):

$$q_t = q_e(1 - \exp^{-k_1 t}) \tag{6}$$

$$q_t = \frac{k_2 q_e^2 t}{1 + k_2 q_e t} \tag{7}$$

The calculated kinetic parameters of all halloysites are given in Table 2. The experimental data were prior analysed by a comparison of calculated q_t against time from these two kinetic models and subsequently determined by linear regression. The first-order kinetic curves of all halloysites did not fit well with the experimental data. While, the pseudo-second-order equation provided an excellent fit between the predicted curves and the experimental data (see Fig. 6(a)). This is confirmed by a good linearization with $R^2 > 0.99$ for all systems (Fig. 6(b)). It may also be found from Table 2 that the calculated q_e values are very close to that of experimentally obtained q_{exp}. Previous results related to the adsorption kinetics of 2.4.5, TCP by different modified clays also support the pseudo-second-order model [10,11]. The initial adsorption rate h_0 (mg/g min) at 298 K was calculated from the pseudo-second-order model parameters with the following equation:

$$h_0 = k_2 q_e^2 \tag{8}$$

and the values are shown in Table 2. It was found that the initial adsorption rate h_0 decreases and follows the sequence: HalCA > HalA > HalAC > HalC. The largest value is obtained for the halloysite HalCA, which probably exhibits more surface and acidity than the other samples.

The diffusion mechanism between adsorbent and adsorbate are not elucidated well by PFO and PSO kinetic models. Weber and Morris [37] described the intraparticle diffusion mechanism between the solutes and particles. Based on this intraparticle diffusion, it can be formulated as follows:

$$q_t = k_3 t^{0.5} + C \tag{9}$$

where C (mg/g) is the intercept related to the boundary layer effect and k_3 (mg/g $min^{0.5}$) is the intraparticle diffusion rate constant. As shown in Table 2, the values of R^2 obtained from the linear regression plots of q_t vs. $t^{0.5}$ (figure not shown) for the whole time data of the sorption process, were low. The low R^2 values suggest that the Weber–Morris model could not describe well the experimental data and that the TCP adsorption process was not limited by the intraparticle diffusion.

Table 2
Kinetic parameters evaluated for TCP adsorption by all halloysite samples

Models	Parameters	samples			
		HalA	HalCA	HalAC	HalC
First-order kinetic model	k_1 (1/min)	0.101	0.125	0.154	0.050
	q_e (mg/g)	3.15	9.58	7.77	3.85
	R^2	0.64	0.586	0.755	0.942
Second-order kinetic model	k_2 (g/mg min)	0.045	0.056	0.102	0.045
	q_e (mg/g)	26.75	36.63	7.42	5.28
	h	32.20	75.13	5.62	1.25
	R^2	0.999	0.999	0.997	0.982
Intraparticle diffusion: whole time data	k_3 (mg/g min$^{0.5}$)	0.866	0.579	0.341	0.54
	C (mg/g)	20.58	32.34	4.95	1.45
	R^2	0.505	0.760	0.751	0.904
Experimental data		26.6	36.5	7.3	6.14

3.5. Equilibrium adsorption isotherms

Fig. 7 shows adsorption isotherms of TCP on the different halloysites in solution of initial pH 2. Isotherms for TCP retention by the all halloysites were similar. The shape of these isotherms is the S-type according to Giles classification [38] for all halloysite samples. For those samples, the isotherms of type S are relatively rare and indicate weak adsorbate–adsorbent interactions. This kind of isotherm implies that adsorption becomes easier as the concentration in the liquid phase increases. Literature shows that S-isotherms are often observed with smectites (essentially montmorillonites) and sometimes also with other clay minerals [39]. Generally, they could be divided into two sections. After the first adsorption step, the increase in the slope of the isotherms at high concentrations may support the cooperative adsorption of adsorbed molecules and the adsorbent becomes more hydrophobic. High retention at the same concentration for 100 mg/L was obtained in the following order: HalCA > HalA > HalC > HalAC. This relationship can probably be explained by the texture (surface area and porosity) of these materials and their acidity. The adsorption equilibrium data of TCP on modified halloysite minerals were fitted applying nonlinear form of Langmuir (Eq. (10)), Freundlich (Eq. (11)) and Toth (Eq. (12)) isotherm models [40].

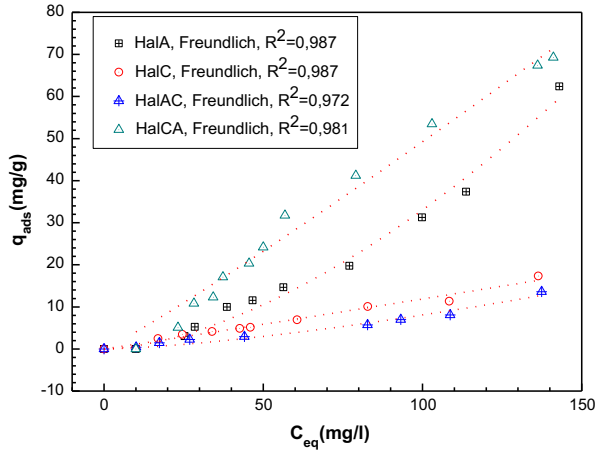

Fig. 7. Isotherms for the equilibrium adsorption data of TCP onto modified halloysite samples (adsorbent mass = 50 mg; T = 23 ± 1°C; V_{agit} = 100 rpm; V_{sol} = 50 mL; pH 2).

$$q_e = \frac{q_m K_L C_e}{1 + K_L C_e} \tag{10}$$

$$q_e = K_F C_e^{1/n} \tag{11}$$

$$q_e = \frac{q_T K_T C_e}{[1 + (K_T C_e)^{m_T}]^{1/m_T}} \tag{12}$$

where q_m (mg/g) is the Langmuir maximum adsorption capacity of the sample and K_L is the Langmuir's constant related to the adsorption energy; K_F is the Freundlich adsorption coefficient and $1/n$ indicates the adsorption intensity and curvature. A $1/n < 1$ represents a normal Langmuir isotherm, whereas $1/n > 1$ indicates cooperative adsorption; q_T (mg/g) and K_T (L/mg) are the Toth constants, representing the monolayer adsorption capacity and the energy of adsorption, respectively, and m_T is an empirical constant.

The applicability of these three models was evaluated by the R^2 values. The highest R^2 values

Table 3
Calculated isotherm parameters for Freundlich model for adsorption of TCP onto halloysites

		Samples			
	Parameters	HalA	HalCA	HalAC	HalC
Freundlich isotherm	k_F (mg/g)(L/mg)$^{1/n}$	0.017	0.335	0.011	0.195
$q_e = K_F C_e^{1/n}$	$1/n$	1.648	1.084	1.432	0.873
	R^2	0.986	0.981	0.972	0.986
Toth isotherm	R^2	0.880	0.974	0.929	0.974
Langmuir isotherm	R^2	0.890	0.976	0.939	0.977

Table 4
Thermodynamic parameters for the adsorption of TCP onto the prepared samples

			ΔG (kJ/mol^{-1})		
Adsorbents	ΔH (kJ/mol^{-1})	ΔS (J/mol^{-1})	278 K	298 K	308 K
HalA	−10.0	8.20	−12.3	−12.44	−12.53
HalCA	21.2	122.4	−12.82	−15.27	−16.50
HalAC	28.0	129.0	−7.86	−10.44	−11.7
HalC	47.8	196.86	−6.93	−10.86	−12.83

determine the best isotherm model by this study. Table 3 compiles the main parameters obtained from the fitting of Freundlich equation, along with the correlation coefficient (R^2) in the case of Toth and Langmuir models. Given the high R^2 values, the adsorption data of TCP on all halloysite samples is better described by the Freundlich model than the Langmuir and Toth models. Freundlich equation gives the evaluation of the adsorption capacity (K_F), as well as the estimation of the affinity adsorbate–adsorbent (parameter $1/n$). The Freundlich constants values ($1/n$ >1) which is a function of the strength of adsorption, suggest that the binding of the TCP onto all halloysite samples was weak and indicated that the removal of TCP on heterogeneous surface of all halloysite samples may involve multilayer adsorption, which also supports the proposed physisorption mechanism [41].

3.6. Thermodynamic study

The temperature is a parameter often investigated in literature and it is shown to affect the transport/kinetic process of TCP adsorption. Thermodynamic parameters such as Gibb's free energy, ΔG_{ads} enthalpy change ΔH_{ads} and change in entropy ΔS_{ads} for the adsorption of TCP on solid adsorbent has been determined using the following equations [42,43]:

$$\Delta G_{ads} = \Delta H_{ads} - T\Delta S_{ads} \quad (13)$$

$$\log\left(\frac{1000 \times q_e}{C_e}\right) = \frac{\Delta S_{ads}}{2.303R} + \frac{-\Delta H_{ads}}{2.303RT} \quad (14)$$

q_e is the amount of TCP adsorbed per unit mass of halloysite (mg/g), C_e is equilibrium concentration (mg/L), m is the adsorbent dose (g/L) and T is temperature in Kelvin. q_e/C_e is called the adsorption affinity. The values of Gibbs free energy ΔG_{ads} had been calculated from the enthalpy of adsorption ΔH_{ads} and the entropy of adsorption ΔS_{ads} and ΔH_{ads} was obtained from the plot of $\log(1000 \times q_e/C_e)$ vs. $1/T$ from Eq. (14). Once these two parameters were obtained, ΔG_{ads} is determined from Eq. (13). The values of ΔH_{ads}, ΔS_{ads} and ΔG_{ads} for the initial TCP concentration of 50 mg/L for all halloysite samples were shown in Table 4. The positive values of ΔS_{ads} suggest the increased randomness at the solid/solution interface during the adsorption. The lower heat ΔH_{ads} of adsorption obtained in this work indicated that physisorptions rather than chemisorptions adsorption was prevailing. The negative values of ΔG_{ads} indicated that the adsorption process was spontaneous.

4. Conclusion

In this work, we have studied the effect of calcination and activation treatment on the structural and chemical properties of an Hal clay. After calcination at 600°C, we observe a complete disappearance of the

XRD peaks, and the structure became amorphous (metakaolin). Acid treatment did not cause much variation in the FTIR spectrum. Surface area was strongly increased by the combination of the thermal and acid treatments. HalCA characterized by the largest specific area, 538.6 m^2/g. The amount of sorption of TCP on halloysite decreased with increasing pH solution. The sorption was rapid during the first 10 min and the equilibrium was reached within 40 min. Kinetics of TCP adsorption onto halloysite fit well the pseudo-second-order model. The best-fit adsorption isotherm was obtained with the Freundlich model. HalCA is a favourable adsorbent for TCP removal from aqueous solutions.

References

[1] Md. Ahmaruzzaman, Adsorption of phenolic compounds on low-cost adsorbents: A review, Adv. Colloid Interface Sci. 143 (2008) 48–67.

[2] H. Zaghouane-Boudiaf, M. Boutahala, Adsorption of 2,4,5-trichlorophenol by organo-montmorillonites from aqueous solutions: Kinetics and equilibrium studies, J. Chem. Eng. 170 (2011) 120–126.

[3] S.G. Poulopoulos, F. Arvanitakis, C.J. Philippopoulos, Photochemical treatment of phenol aqueous solutions using ultraviolet radiation and hydrogen peroxide, J. Hazard. Mater. 129 (2006) 64–68.

[4] P. Canizares, J. Lobato, R. Paz, M.A. Rodrigo, C. Saez, Electrochemical oxidation of phenolic wastes with boron-doped diamond anodes, Water Res. 39 (2005) 2687–2703.

[5] J.L. Acero, F.J. Benitez, A.I. Leal, F.J. Real, Removal of phenolic compounds in water by ultrafiltration membrane treatments, J. Environ. Sci. Health Part A Toxic/Hazard. Subst. Environ. Eng. 40 (2005) 1585–1603.

[6] B.H. Hameed, I.A.W. Tan, A.L. Ahmad, Adsorption isotherm, kinetic modeling and mechanism of 2,4,6-trichlorophenol on coconut husk-based activated carbon, Chem. Eng. J. 144 (2008) 235–244.

[7] Q. Zhou, H.P. He, J.X. Zhu, W. Shen, R.L. Frost, P. Yuan, Mechanism of p-nitrophenol adsorption from aqueous solution by HDTMA+-pillared montmorillonite—Implications for water purification, J. Hazard. Mater. 154 (2008) 1025–1032.

[8] L.Z. Zhu, R.L. Zhu, Simultaneous sorption of organic compounds and phosphate to inorganic–organic bentonites from water, Sep. Purif. Technol. 54 (2007) 71–76.

[9] R.S. Juang, S.H. Lin, K.H. Tsao, Mechanism of sorption of phenols from aqueous solutions onto surfactant-modified montmorillonite, J. Colloid Interface Sci. 254 (2002) 34–241.

[10] H. Zaghouane-Boudiaf, M. Boutahala, Kinetic analysis of 2,4,5-trichlorophenol adsorption onto acid-activated montmorillonite from aqueous solution, Int. J. Miner. Process. 100 (2011) 72–78.

[11] H. Zaghouane-Boudiaf, M. Boutahala, Preparation and characterization of organo-montmorillonites. Application in adsorption of the 2,4,5-trichlorophenol from aqueous solution, Adv. Powder Technol. 22 (2011) 735–740.

[12] S.R. Levis, P.B. Deasy, Characterisation of halloysite for use as a microtubular drug delivery system, Int. J. Pharm. 243 (2002) 125–134.

[13] S. Mellouk, S. Cherifi, M. Sassi, K. Marouf-Khelifa, A. Bengueddach, J. Schott, A. Khelifa, Intercalation of halloysite from Djebel Debagh (Algeria) and adsorption of copper ions, Appl. Clay Sci. 44 (2009) 230–236.

[14] M. Zhao, P. Liu, Adsorption behavior of methylene blue on halloysite nanotubes, Microporous Mesoporous Mater. 112 (2008) 419–424.

[15] Y. Li, Q.-Y. Yue, B.-Y. Gao, Effect of humic acid on the Cr(VI) adsorption onto Kaolin, Appl. Clay Sci. 48 (2010) 481–484.

[16] A.R. Tehrani-Bagha, H. Nikkar, N.M. Mahmoodi, M. Markazi, F.M. Menger, The sorption of cationic dyes onto Kaolin: Kinetic, isotherm and thermodynamic studies, Desalination 266 (2011) 274–280.

[17] K. Backfolk, J.B. Rosenholm, J. Husband, D. Eklund, The influence of surface chemical properties of kaolin surfaces on the adsorption of poly(vinyl alcohol), Colloids Surf., A: Physicochem. Eng. Aspects 275 (2006) 133–141.

[18] G. Suraj, C.S.P. Iyer, M. Lalithambika, Adsorption of cadmium and copper by modified kaolinites, Appl. Clay Sci. 13 (1998) 293–306.

[19] S. Brunauer, P.H. Emmett, E. Teller, Adsorption of gases in multimolecular layers, J. Am. Chem. Soc. 60 (1938) 309–319.

[20] E.P. Barrett, L.G. Joyner, P.H. Halenda, The determination of pore volume and area distributions in porous substances. I. Computations from nitrogen isotherms, J. Am. Chem. Soc. 73 (1951) 373–380.

[21] B.K. Nandi, A. Goswami, M.K. Purkait, Adsorption characteristics of brilliant green dye on kaolin, J. Hazard. Mater. 161 (2009) 387–395.

[22] F. Bergaya, M. Vayer, CEC of clays: Measurement by adsorption of a copper ethylenediamine complex, Appl. Clay Sci. 12 (1997) 275–280.

[23] K.G. Bhattacharyya, S.S. Gupta, Influence of acid activation on adsorption of Ni(II) and Cu(II) on kaolinite and montmorillonite: Kinetic and thermodynamic study, Chem. Eng. J. 136 (2008) 1–13.

[24] C. Belver, M.A. Bañares, M.A. Vicente, Preparation of porous silica by acid activation of metakaolins, Stud. Surf. Sci. Catal. 144 (2002) 307-314.

[25] R.M. Torres Sánchez, E.I. Basaldella, J.F. Marco, The effect of thermal and mechanical treatments on kaolinite: characterization by XPS and IEP measurements: J. Colloid Interface Sci. 215 (1999) 339–344.

[26] A.G. San Cristobal, R. castello, M. Angeles Martin Luengo, C. Vizcayno, Acid activation of mechanically and thermally modified kaolins, Mater. Res. Bull 44 (2009) 2103–2111.

[27] K.P. Nicolini, C.R.B. Fukamachi, F. Wypych, A.S. Mangrich, Dehydrated halloysite intercalated mechanochemically with urea: Thermal behavior and structural aspects, J. colloid Interface Sci. 338 (2009) 474–479.

[28] G. Tarì, I. Bobos, C.S.F. Gomes J.M.F. Ferreira, Modification of surface charge properties during kaolinite to halloysite-7Å transformation, J. Colloid Interface Sci. 210 (1999) 360–366.

[29] M. Castellano, A. Turturro, P. Riani, T. Montanari, E. Finocchio, G. Ramis, G. Busca, Bulk and surface properties of commercial kaolins, Appl. Clay Sci. 48 (2010) 446–454.
[30] A.G. San Cristobal, R. castello, M. Angeles Martin Luengo, C. Vizcayno, Zeolites prepared from calcined and mechanically kaolins. A comparative study, Appl. Clay Sci. 49 (2010) 239–246.
[31] S.J. Gregg, K.S.W. Sing, Adsorption, Surface Area and Porosity, Academic Press, New York, NY, 1991.
[32] B.H. Hameed, Equilibrium and kinetics studies of 2,4,6-trichlorophenol adsorption onto activated clay, Colloids Surf., A: Physicochem. Eng. Aspects 307 (2007) 45–52.
[33] M. Radhika, K. Palanivelu, Adsorptive removal of chlorophenols from aqueous solution by low cost adsorbent—Kinetics and isotherm analysis, J. Hazard. Mater. 138 (2006) 116–124.
[34] R. Gao, J. Wang, Effects of pH and temperature on isotherm parameters of chlorophenols biosorption to anaerobic granular sludge, J. Hazard. Mater. 145 (2007) 398–403.
[35] S.Y. Lagergren, Zur Theorie der Sogenannten adsorption geloester Stoffe, (on the theory of so-called adsorption of solutes), K. Sven. Vetenskapsakad. Handl. 24 (1898) 1–39.
[36] Y.S. Ho, G. McKay, Pseudo-second-order model for sorption processes, Process Biochem. 34 (1999) 451–465.
[37] W.J. Weber, J.C. Morris, Kinetics of adsorption on carbon from solution. J. Sanitary Eng. Div. Am. Soc. Civil Eng. 89 (1963) 31–60.
[38] C.H. Giles, T.H. MacEwan, S.N. Nakhwa, D. Smith, 786. Studies in adsorption. Part XI. A system of classification of solution adsorption isotherms, and its use in diagnosis of adsorption mechanisms and in measurement of specific surface areas of solids, J. Chem. Soc. 111 (1960) 3973–3993.
[39] R. Calvet, Adsorption of organic chemicals in soils, Environ. Health Perspect. 83 (1989) 145–177.
[40] D.D. Do, Adsorption Analysis: Equilibria and Kinetics, Chemical Engineer Series, vol. 2, Imperial College Press, London, 1998.
[41] V.O. Njoku, M.A. Islam, M. Asif, B.H. Hameed, Preparation of mesoporous activated carbon from coconut frond for the adsorption of carbofuran insecticide, J. Anal. Appl. Pyrolysis 110 (2014) 172–180.
[42] S. Canzano, P. Iovino, S. Salvestrini, S. Capasso, Comment on "Removal of anionic dye Congo red from aqueous solution by raw pine and acid-treated pine cone powder as adsorbent: Equilibrium, thermodynamic, kinetics, mechanism and process design", Water Res. 46 (2012) 4314–4315.
[43] S. Dawood, T.K. Sen, "Author's responses to the comment by Canzano et al. and also corrigendum to Removal of anionic dye Congo red from aqueous solution by raw pine and acid-treated pine cone powder as adsorbent: Equilibrium, thermodynamic, kinetics, mechanism and process design" published in Water Research, vol. 46, pp. 1933–1946, 2012 Water Res. 46 (2012) 4316–4317.